Arch Clin Infect Dis. 2023 February; 18(1):e135078. https://doi.org/10.5812/archcid-135078.

Published online 2023 May 13. **Research Article**

Adipose-derived Stem Cells Improving Inflammatory and Proliferative Responses in an Infected and Ischemic Ulcer Model in Type 1 Diabetic Rats: Insights Into Bacterial Count, Stereological Parameters, microRNA-21, and FGF2 Regulation

Abdollah Amini [1, *], Melika Farzin [1], Masoumeh Hajihosseintehrani [1] and Mohammad Bayat [2, 3, 1, **]

[1] Department of Biology and Anatomical Sciences, Shahid Beheshti University of Medical Sciences, Tehran, Iran
[2] Price Institute of Surgical Research, University of Louisville, Louisville, USA
[3] Noveratech LLC, Louisville, USA

[*] *Corresponding author*: Department of Biology and Anatomical Sciences, Shahid Beheshti University of Medical Sciences, Tehran, Iran. Email: d.amini2008@yahoo.com
[**] *Corresponding author*: Price Institute of Surgical Research, University of Louisville, Louisville, USA. Email: bayat_m@yahoo.com

Received 2023 January 22; **Revised** 2023 April 26; **Accepted** 2023 April 26.

Abstract

Background: Adipose-derived stem cells (ADSCs) have been shown to enhance wound healing in rats with type 1 diabetes (DM1).
Objectives: This experimental study aimed to explore how ADSC administration affects bacterial count, wound size, biomechanical and stereological parameters, and the expression of microRNA-21 and FGF2 in a rat model of infected, ischemic, and delayed wound healing in DM1.
Methods: Twenty-four male adult Wistar rats weighing less than 250 g were randomly assigned to four groups (n = 6 per group). Type 1 diabetes was induced in all animals, resulting in the development of a delayed, ischemic, and infected wound model. The CG_{day4} and CG_{day8} groups served as controls. In the AG_{day4} group, the animals received allograft h-ADSs and were euthanized on day four after surgery. Similarly, in the AGday8 group, the animals received h-ADSs and were euthanized on day eight after surgery. Microbial colony counts, wound size, stereological parameters, and the expression of microRNA-21 and FGF2 were evaluated in this study during the inflammation (day 4) and proliferation (day 8) stages of wound healing.
Results: We demonstrated that h-ADSs significantly reduced microbiological counts compared to the control group on days 4 and 8. Moreover, in the AG_{day8} group compared to the AG_{day4} group, this decline in microbiological counts was even more pronounced. Moreover, we observed that the stereological characteristics in the AG_{day4} and AG_{day8} groups were significantly superior to those in the CG groups. Additionally, the AG_{day4} and AG_{day8} groups exhibited smaller ulcer area sizes compared to the CG groups. Furthermore, the AG_{day4} and AG_{day8} groups demonstrated higher expression levels of FGF2 and microRNA-21 than the CG groups on days 4 and 8. Notably, on day 8, the AG_{day8} group's outcomes surpassed those of the AG_{day4} group ($P < 0.01$).
Conclusions: Through lowering microbial counts, modifying stereological parameters, microRNA-21, and FGF2 expression, the administration of hADS dramatically speeds up the healing of MARS-infected and ischemic ulcers in DM1 rats.

Keywords: Type One Diabetes Mellitus, Ulcer Healing, Adipose-derived Stem Cells, Stereological Parameters, Microbial Examination, Wound Area Measurement, Rats

1. Background

Insufficient production of insulin by the pancreas leads to type 1 diabetes (DM1), which is a chronic condition (1). In 2017, there were 451 million reported cases of diabetes worldwide, with a projected increase to 693 individuals with DM1 by 2045. Among the significant challenges faced by DM1 patients, an elevated risk of diabetic foot ulcers (DFUs) is prominent. DFUs arise from the interplay of several relevant factors, namely infection, ischemia, and neuropathy, which are the primary pathogenic causes of diabetic foot complications. Evidence suggests that lower limb amputation occurs in approximately 75% to 85% of cases subsequent to foot ulcers, which are commonly linked to chronic infection. These ulcers are characterized by reduced recruitment of endothelial progenitor cells (EPCs), impaired angiogenesis, decreased proliferation and migration of skin cells such as keratinocytes and fibroblasts, and heightened inflammatory cell presence (2).

In diabetes wounds, the parenchyma surrounding the wound, comprising fibroblasts, myofibroblasts, inflammatory cells, new blood vessels, regenerated neurons, and other cell types, undergoes detrimental changes (3). In response to tissue damage, fibroblast, endothelial, and macrophage cells, particularly endothelial cells (EC), secrete basic fibroblast growth factor (FGF-2), which plays a critical role in promoting wound healing (4, 5). Several studies have demonstrated the potential of FGF-2 in accelerating the healing process of diabetic wounds and its promise as a therapy for diabetic ulcers (4, 5).

Basic fibroblast growth factor (bFGF), also referred to as FGF2 plays a protective role by preventing endothelial cell death and promoting endothelial cell proliferation and angiogenesis. The signaling pathways involving FGF and microRNA (miRNA) have been demonstrated to influence various cellular processes, such as cell specification, proliferation, migration, differentiation, and survival (6).

MicroRNAs are non-coding RNAs that regulate gene expression.

Recent research indicates that miRNAs play a substantial role in both normal healing processes and the etiology of chronic ulcers, such as DFUs (7). Among the earliest mammalian miRNAs discovered, microRNA-21 (miR-21) has been found to participate in numerous biological activities. Increasing evidence suggests that miR-21 plays a crucial role in cutaneous injury and skin wound healing by forming intricate networks with its target genes and signaling pathways (8). The therapeutic effectiveness of miR-21 may be attributed to its ability to enhance fibroblast differentiation, promote angiogenesis, exert anti-inflammatory effects, enhance collagen synthesis, and facilitate wound re-epithelialization. Xie et al. discovered that miR-21 inhibits inflammation and promotes wound healing by modulating NF-κB expression through PDCD4 and FGF pathways (8). However, in diabetic wounds, the expression of miR-21 is significantly lower (8). Reduced miR-21 levels are also associated with increased expression of its target genes (9-11). As a result, increasing the levels of miRNA-21 in damaged tissue can effectively reduce inflammatory signals and enhance the healing process (11, 12). In essence, it is now acknowledged that over 100 molecules contribute to impaired skin healing in a non-conventional manner among individuals with diabetes (13). The use of appropriate medications and biomodulators appears to hold promise in the treatment of non-healing ulcers (14).

Mesenchymal stem cells (MSCs) have emerged as a valuable and effective treatment for skin wounds in contemporary medicine. Their remarkable differentiation potential, minimal immunogenicity, ease of collection, and significant contribution to the natural wound healing process make them an attractive therapeutic option.

Adipose tissue-derived mesenchymal stem cells (AD-MSCs) expedite the healing process of skin wounds through various mechanisms. These include promoting angiogenesis, granulation, and epithelialization, reducing inflammation, facilitating cell migration, and aiding in the reconstruction of the extracellular matrix (ECM) in tissues. The presence of AD-MSCs contributes to the establishment of favorable microenvironments for regenerative wound healing (15, 16). The extraction of adipose-derived stem cells (ADSCs) from adipose tissue and their subsequent in vitro expansion are straightforward processes. Preclinical investigations have demonstrated that ADSCs possess the ability to expedite the healing of wounds in diabetic patients. This is achieved through enhancements in epithelialization and granulation tissue formation, as well as the release of anti-apoptotic, anti-inflammatory, and angiogenic cytokines (17).

To the best of our knowledge, no previous studies have examined the impact of human adipose-derived stem cells (hADSCs) on the bacterial count, stereological parameters, and the expression of microRNA-21 and FGF2 in a model of infected, ischemic, and delayed wound healing in rats with DM1.

2. Objectives

Our study aimed to investigate the effects of hADSC administration on the bacterial count, stereological parameters, microRNA-21 expression, FGF2 expression, and wound size in a model of infected, ischemic, and delayed wound healing in rats with DM1.

3. Methods

3.1. Animals and Study Design

Twenty-four male Wistar rats, aged three months, were randomly divided into four groups (n = 6 per group). Type 1 diabetes was induced in all experimental animals. A model of delayed, ischemic, and MARS-infected wounds was created in all experimental animals. The experimental animals were allocated into four groups as follows: CG_{day4} and CG_{day8}, which served as control groups 1 and 2, respectively. The hAG_{day4} group consisted of rats that received allograft hADSCs and were euthanized four days after surgery. The hAGday8 group received hADSCs and were euthanized on day eight after surgery.

In this study, we evaluated the wound area, microbial colony counts, stereological examination, and the expression of FGF2 and miR-21 on days 4 (inflammation phase) and 8 (proliferation phase), respectively.

The experiment was approved by the Medical Ethics Department of the School of Medicine, Shahid Beheshti University of Medical Sciences (SBMU), Tehran, Iran (file no. IR.SBMU.MSP.REC.1400.295).

3.2. Separation, Expansion, and Immunophenotyping of Allograft h-ADS

Human adipose tissue was obtained from the subcutaneous tissue of a healthy 38-year-old woman who underwent mammoplasty surgery, following informed consent from the patient. Approximately 5 cc of adipose tissue was manually crushed and subsequently washed in PBS containing penicillin and streptomycin. The tissue was then digested using a 0.1% collagenase-I solution for 40 - 60 minutes at 37°C, followed by centrifugation. Red blood cells were removed using a lysis buffer. The cell pellets were then resuspended in Dulbecco's modified eagle medium (DMEM) supplemented with 20% fetal bovine serum (FBS) and transferred into T-75 flasks containing DMEM supplemented with 20% FBS, 100 U/mL penicillin, and 100 μg/mL streptomycin. The expression of MSC markers in ADSs was evaluated using flow cytometry, following the previously described methods (18, 19).

3.3. ADS Transplantation

A total of 1×10^6 ADSs from passage four were intradermally transplanted into eight areas surrounding the ulcer, approximately 4 - 5 mm from the edge of the ulcer (Figure 1).

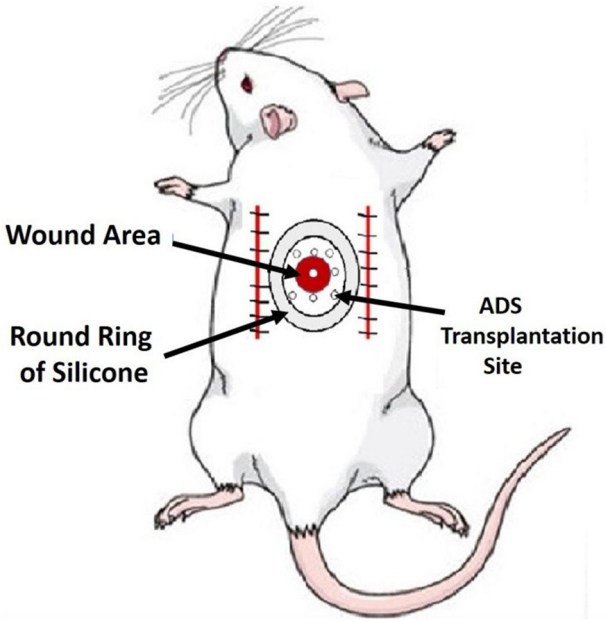

Figure 1. Photograph of the wound area and adipose-derived stem cell injection site (ADS) in the rats

3.4. DM1 Induction

DM1 was induced using a single intraperitoneal injection of streptozotocin (STZ) at a dose of 40 mg/kg (20). One week after the STZ injection, blood samples were collected to measure blood sugar levels. DM1 was defined as blood sugar levels exceeding 250 mg/dL. All rats with DM1 were monitored for 30 days to confirm the induction of DM1 (20).

3.5. Clinical Tests

The body weight and blood glucose levels of DM1 rats were monitored throughout the experiment.

3.6. Surgery

Rats were anesthetized using 50 mg/kg of ketamine and 5 mg/kg of xylazine. Prior to surgery, all treated rats received ceftriaxone at a dose of 50 mg/kg, which was continued for 24 and 48 hours post-surgery. A dorsal, bipedicle skin flap measuring $10 \times 3 \times 5$ cm was created on the dorsal skin of all rats. A 12-mm full-thickness excisional round ulcer was then generated at the midpoint of the flap using a biopsy punch. A round piece of silicone was sutured using a 0.4 silk skin holder to secure the skin lesion. Additionally, all experimental rats were administered 20 mg/kg of ibuprofen every 8 - 12 hours before and for five days after surgery (Figure 1).

3.7. Injection of MRSA into the Ulcer Area and Microbiological Test

In this study, the MRSA strain (ATCC 25923) was utilized. The methodology for this strain has been previously described. In summary, a colony of MRSA with a concentration of 2×10^8 at 1 cc was prepared. A 100-l aliquot (2×10^7 MRSA) was locally injected into all ulcers following surgery.

For microbiological tests, samples were collected from the injured areas on days 0, 4, and 8, respectively. The bacterial colonies were then counted as the number of bacteria per sample (colony-forming units (CFUs)) (21, 22).

3.8. Wound Area Measurement (WAM)

In this study, a digital camera was used to capture photographs of the wound site on days 0, 4, and 8. The size of the wounds (measured in mm^2) was then determined using Image J-NIH software (USA) and compared to the measurements taken on day zero (23).

3.9. Wound Strength Examination

On day 16, a 50 mm × 5 mm sample was collected from each wound site and placed in a material testing machine. The rate of deformation was set at 10 mm/min. The maximal force (N) and stress under high load (N/cm^2) of the samples were determined from the load-deformation curve (21).

3.10. Histological and Stereological Analysis

The skin samples obtained from the wound areas were initially fixed in formalin solutions. Paraffin-embedded tissue blocks were prepared, and serial sections of 5-μm thickness were cut. These sections were then stained using a standard laboratory staining method. The numerical density (Nv) of neutrophils, macrophages, fibroblasts, and blood vessels in each wound area was subsequently calculated.

Cell count estimation:

$$Nv = \frac{\Sigma Q}{h \times \frac{a}{f} \times \Sigma p} \quad (1)$$

ΣQ = the number of cells; h = dissector height; a/f = the entire area of the counted frames; and ΣP = the total number of counting frames.

Number of blood vessels:

$$Number\ of\ blood\ vessels = \frac{2\Sigma Q}{\Sigma P \times \frac{a}{f}} \quad (2)$$

where ΣQ = all vessel numbers counted per wound. The number of blood vessels was considered a marker for angiogenesis.

3.11. RNA Extraction and Quantitative Real-time Polymerase Chain Reaction Detection of miR-21 Expression Level

Initially, skin wound samples were obtained from the designated areas on the rats. Subsequently, total RNA was extracted from these skin samples using Trizol (Invitrogen, Carlsbad, CA).

The obtained total mRNA was assessed for purity using a Bioanalyzer 2100 (Agilent Technologies, Inc., Santa Clara, CA) by measuring the absorbance ratio at 260/280 nm. Subsequently, the purified total mRNAs were stored in a nitrogen tank at -80°C. For reverse transcription, cDNA reverse transcription kits (Applied Biosystems, Carlsbad, CA) were used.

After pre-amplification, the expression levels of the target genes were evaluated using SYBR Green and quantitative real-time polymerase chain reaction (qRT-PCR) on a StepOne™ thermal cycler (Applied Biosystems). GAPDH was used as a housekeeping gene, and RNU6b (RNA, U6 small nuclear 2) served as a reference gene. The primer lists for GAPDH, FGF2, microRNA21, and RNU6b can be found in Table 1. The gene expression level in the studied rats was calculated using the REST 2009 software, employing the Pair Wise Fixed Reallocation Randomization Test. The obtained data were analyzed using the ΔΔCT and Pfaffl methods for comparison.

Table 1. The Primer Sequences of the Studied Genes

Target Gene	Primer Sequence	Tm
FGF2		
F	GACCCACACGTCAAACTACA	57.77
R	GCCGTCCATCTTCCTTCATAG	58.24
GAPDH		
F	ATCTGACATGCCGCCTGGAG	61.40
R	AAGGTTGGAAGAATGGGAGTTGC	60.25
microRNA-21		
F	CGCCCGTAGCTTATCAGA	62.10
PROB	TGCATACGACTCAACATC	59.14
RNU6 small nuclear 2		
F	GTGCTCGCTTCGGCAGCACATAT	64.40
PROB	TGTATCGTTCCAATTT TATCGGATGT	63.05

Abbreviations: FGF2, fibroblast growth factor 2; GAPDH, glyceraldehyde 3-phosphate dehydrogenase; RNU6, RNA, U6 small nuclear 2.

3.12. Statistical Analysis

The collected data were analyzed using SPSS version 21, and the results were reported as the mean ± standard deviation (SD). Statistical analysis of the data obtained from body weight measurements, microbiological tests, wound strength tests, and wound area size involved the use of *t*-tests, one-way analysis of variance (ANOVA), and the least significant difference (LSD) test. A significance level of $P < 0.05$ was considered statistically significant.

4. Results

4.1. The Expression of the Stem Cell Marker

The results obtained from flow cytometry analysis revealed that ADSs expressed CD11b (0.21%) and CD45 (0.66%). Furthermore, CD44 and CD105 were found to be fully expressed (100%) by ADSs (Figure 2).

4.2. Clinical Observations

Clinical evidence revealed that all rats exhibited DM1, as indicated by a significant increase in blood sugar levels

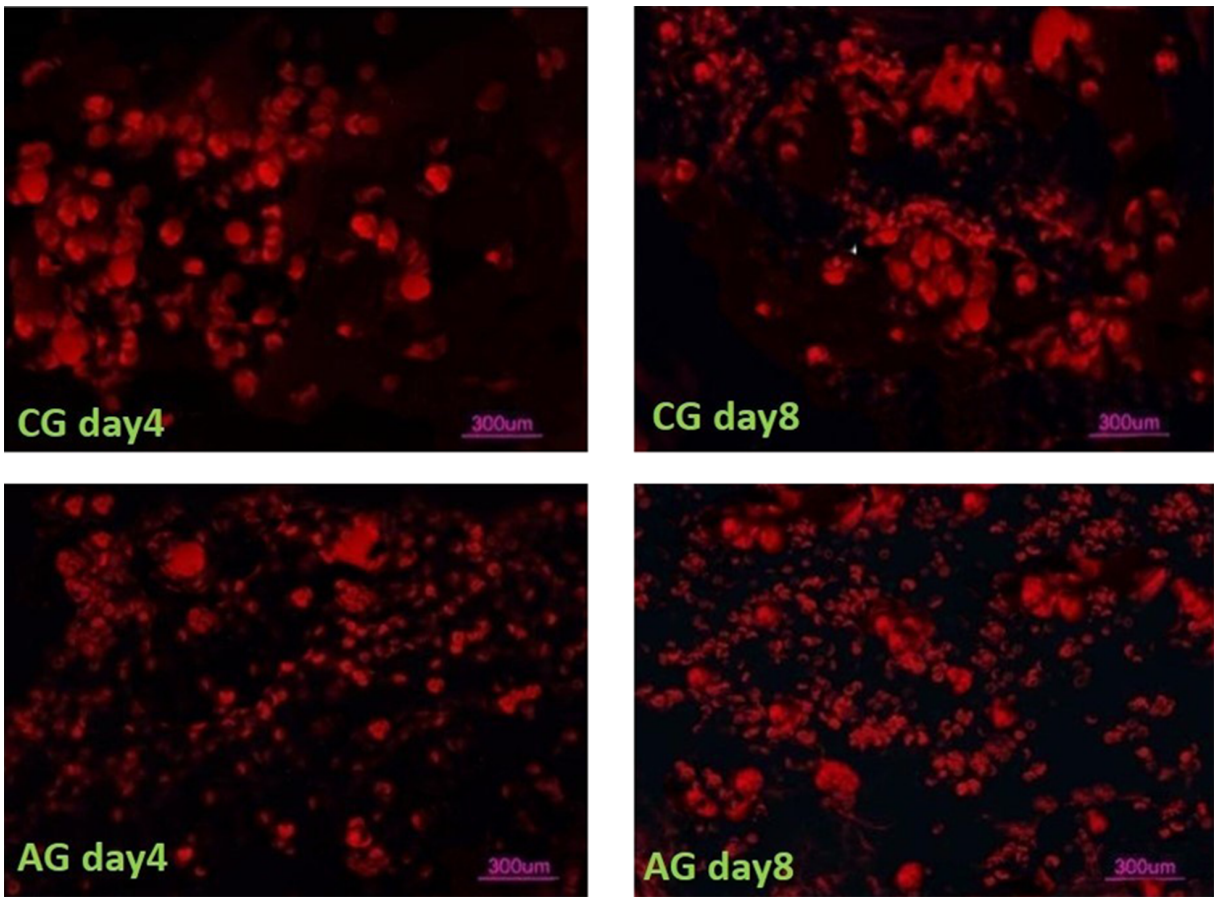

Figure 2. Red fluorescent CM-DiI-labeled human-derived mesenchymal stem cells were revealed in the rat skin wound regions of all the studied groups on days 4 and 8 after surgery. CG, control group; AG, adipose-derived stem cell treatment group.

Table 2. The Blood Sugar and Body Weight of the Studied Groups were Evaluated and Compared Using a Student's *t*-test [a]

Groups Factors	Control	ADS
First blood sugar (mg/dL)	455.02 ± 52.3	401.02 ± 34
Final blood sugar(mg/dL)	384.3 ± 63.74 [b]	250 ± 31.2
First body weight(g)	310.4 ± 12.6	300.75 ± 19.14
Final body weight(g)	265.75 ± 15.95 [c]	246.5 ± 14.26 [c]

[a] Values are expressed as mean ± SD.
[b] $P < 0.01$
[c] $P < 0.05$

and a decrease in body weight following STZ treatment (Table 2). The results of our independent *t*-test indicated a significantly higher body weight in the hAG groups compared to the respective control group ($P = 0.005$).

The hAG group showed a significant improvement in blood sugar levels, with a more pronounced decrease compared to the control group.

4.3. Microbial Findings

4.3.1. Day 4

Our microbial study showed that the level of colony-forming units (CFUs) was significantly lower in the hAG_{day4} group ($P = 0.000$) compared to the CG_{day4} group (Figure 3). Similarly, there were significant changes in the CFU count between the hAG_{day8} group and the CG_{day8} group ($P = 0.004$).

The changes in the CFU count were significantly greater in the hAGday8 group compared to the hAG_{day4} group ($P = 0.001$) (Figure 3).

4.4. Wound Area Measurement (WAM)

4.4.1. Day 4

On days 4 and 5, the wound area in the AG_{day4} experimental group was significantly larger than that in the CG_{day4} control group ($P = 0.009$) (Figure 4).

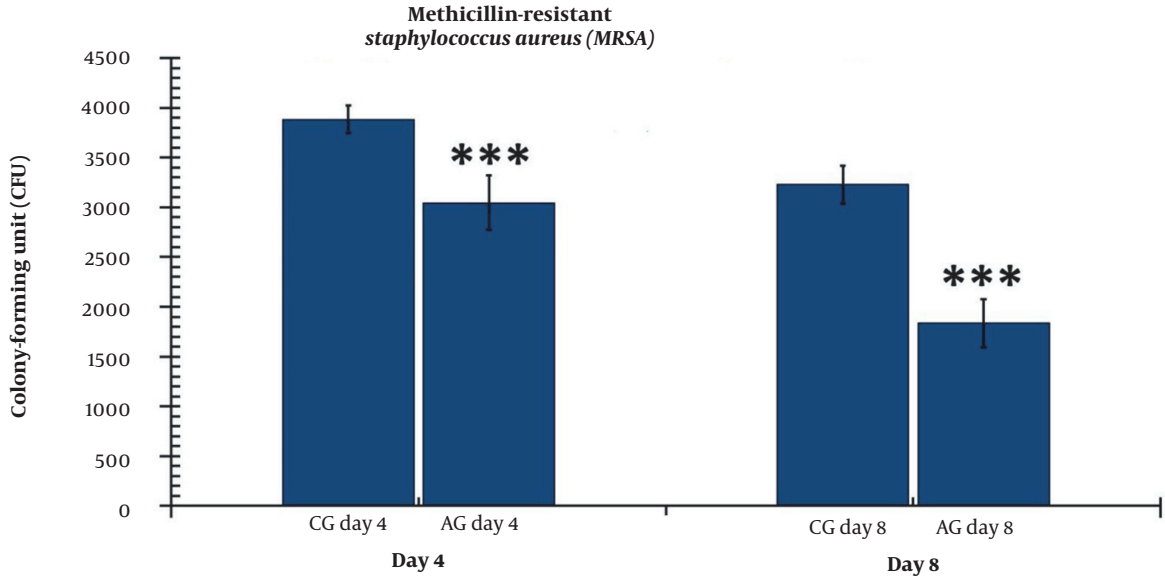

Figure 3. The number of colony-forming units (CFUs) in the experimental and control groups on days 4 and 8. The independent-samples *t*-test and least significant difference (LSD) tests were used to examine the results, which were shown as a mean ± SD. * refers to $P < 0.05$, ** refers to $P < 0.01$, and *** refers to $P < 0.001$. CG, control group; AG, human adipose-derived stem cell group.

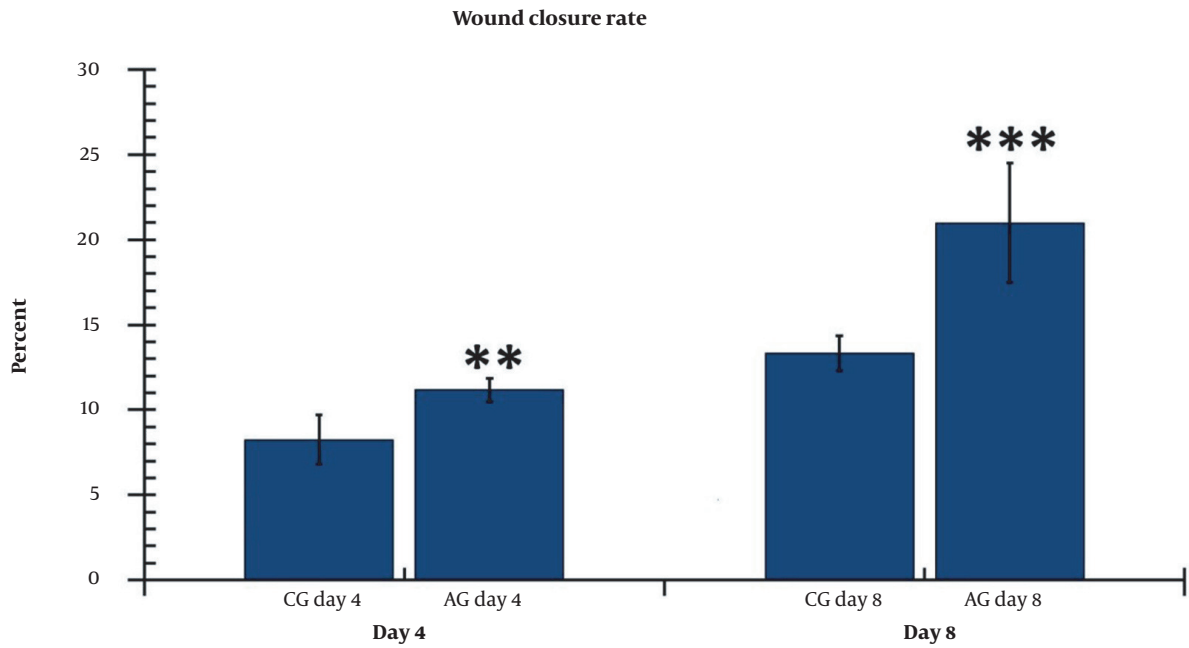

Figure 4. The size of the wound area on days 4 and 8 in the study groups. The Independent-samples *t*-test and LSD tests were used to examine the data. ** and *** denote a P value of less than 0.01 and 0.001, respectively. CG, control group; AG, human adipose-derived stem cell group.

4.4.2. Day 8

The wound area size was significantly smaller in the hAG_{day8} groups (P = 0.001) compared to the CG_{day8} groups. The results in the hAG_{day8} groups exhibited a greater reduction in wound area compared to the hAG_{day4} group (P = 0.021) (Figure 4).

4.5. Tensiometric Examination

All P-values were correlated with the LSD test. Tensiometric examination results are shown in Figure 5.

The level of stress high load in the treatment group (AG) was significantly higher than in the control group (P = 0.01) (Figure 5A). Additionally, the level of maximum energy absorption in the AG group was significantly improved compared to the CG (P = 0.04) (Figure 4B).

4.6. Stereological Findings

Figures 6 - 8 display the stereological findings for all studied groups on days 4 and 8. In terms of the stereological study, it was observed that on both days 4 and 8, all experimental groups exhibited superior stereological results compared to the control group. Furthermore, significant improvements were observed in the hAG_{day8} treatment group compared to the hAG_{day4} group ($P < 0.05$).

4.7. Fibroblast Count

Figure 7A illustrates the fibroblast findings in the studied groups on days 4 and 8. On both days 4 and 8, the experimental groups exhibited a higher number of fibroblasts compared to the control group (P = 0.016 for day four and P = 0.000 for day 8). Additionally, a significant increase in fibroblasts was observed in the hAG_{day8} treatment group compared to the hAG_{day4} group (P = 0.017).

4.8. Angiogenesis

Figure 7B demonstrates that the hAG_{day4} and hAG_{day8} groups had significantly more blood vessels than the CG_{day4} and CG_{day8} groups on day 4 (P = 0.000, P = 0.003) and day 8 (P = 0.041, P = 0.003), respectively. Additionally, the number of blood vessels in the CG_{day8} group was significantly lower compared to the hAG_{day8} group (P = 0.037).

4.9. Neutrophils Count

Figure 8A illustrates the neutrophil findings in the studied groups on days 4 and 8. On both days 4 and 8, the experimental groups exhibited significantly lower levels of neutrophils compared to the control group (P = 0.013 for day four and P = 0.000 for day 8). Furthermore, we observed fewer neutrophils in the hAG_{day8} treatments compared to hAG_{day4} (P = 0.01).

4.10. Macrophage Count

Figure 8B illustrates the macrophage findings in the studied groups on days 4 and 8. On both days 4 and 8, the experimental groups exhibited significantly lower levels of macrophages compared to the control group (P = 0.008 for day four and P = 0.010 for day 8).

4.11. The Expression Level of FGF2

On day 4, the CG_{day4} groups exhibited significantly higher levels of FGF2 (P = 0.008) compared to the control group (P = 0.024). Furthermore, the hAG_{day8} group demonstrated higher levels of FGF2 compared to the CG-day8 group (P = 0.002), as shown in Figure 9A.

4.12. The Gene Expression Level of miR-21

Figure 9B displays the gene expression levels of miR-21 in the wound bed on days 4 and 8.

On day 4, the levels of miR-21 in the hAG_{day4} group were significantly higher than in the control group (P = 0.007). On day 8, the level of miR-21 in the hAG_{day8} group was also significantly higher than in the control group (P = 0.003). Moreover, the findings of the hAG_{day8} group were significantly more pronounced than those of hAG_{day4} (P = 0.010).

5. Discussion

In this study, we aimed to assess the therapeutic effects of hADS on the bacterial count, stereological parameters, expression of microRNA-21, FGF2, and ulcer size in a rat model of infected, ischemic, and delayed wound healing in DM1. Overall, our findings demonstrate that both experimental groups (hAG_{day4} and hAG_{day8}) exhibited substantial reductions in microbial flora counts, improved wound closure rates, and increased expression of microRNA-21 and FGF2 on days 4 and 8. Additionally, the hAG_{day8} group showed significantly more pronounced effects on stereological parameters compared to the other groups.

There are numerous promising advancements in cell therapy and tissue engineering, offering potential therapeutic options for addressing the challenges associated with impaired skin healing, including DFUs (22, 24).

In recent years, stem cell therapy has emerged as a novel therapeutic approach for addressing various conditions, including impaired wound healing and tissue regeneration. Several types of stem cells, including ADSCs, bone marrow-derived mesenchymal stem cells (BM-MSCs), endothelial progenitor cells, keratinocytes, and human skin fibroblasts, have been utilized in both clinical and preclinical settings to enhance wound repair. Among these, mesenchymal ADSCs have gained significant attention due to

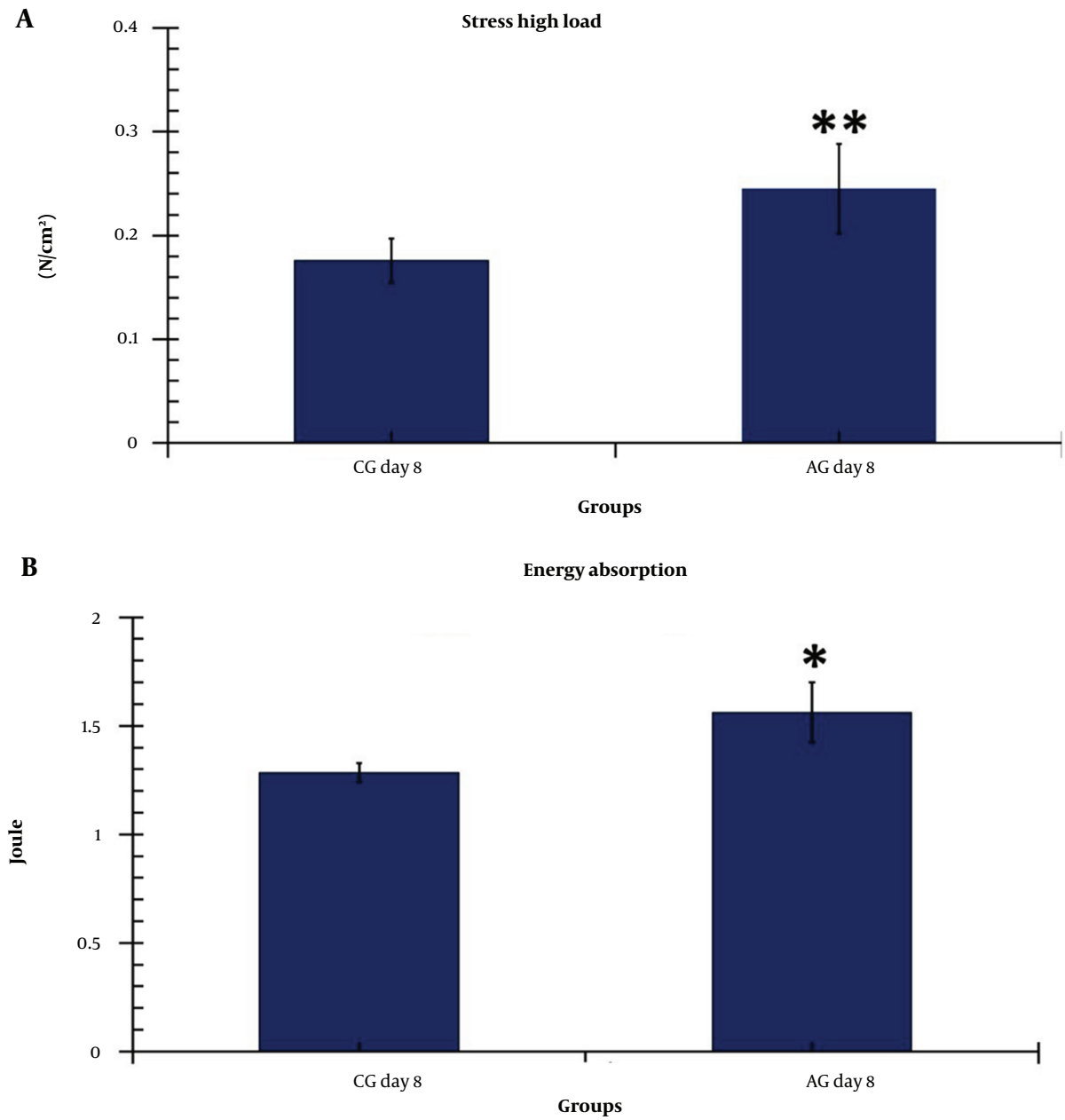

Figure 5. A, Comparison of stress high load; and B, Energy absorption of the wounds in the study groups according to the independent *t*-test. * $P < 0.05$; ** $P < 0.01$. CG, control group; AG, human adipose-derived stem cell group.

their abundance and demonstrated efficacy in promoting wound healing.

Due to their abundant adipose tissue content, extensive ex vivo proliferative capacity, ease of isolation, and ability to secrete pro-angiogenic growth factors while minimizing immunological reactions, adipose tissue cells have emerged as a readily accessible and preferred cell source for therapeutic applications in the management of chronic non-healing wounds (25-27). Transplantation of ADSCs has enhanced neovascularization and improved blood flow in ischemic tissues in murine models (28, 29).

Additionally, studies have demonstrated that ADSCs contribute to arteriogenesis in ischemic tissue through paracrine signaling pathways facilitated by the secretion

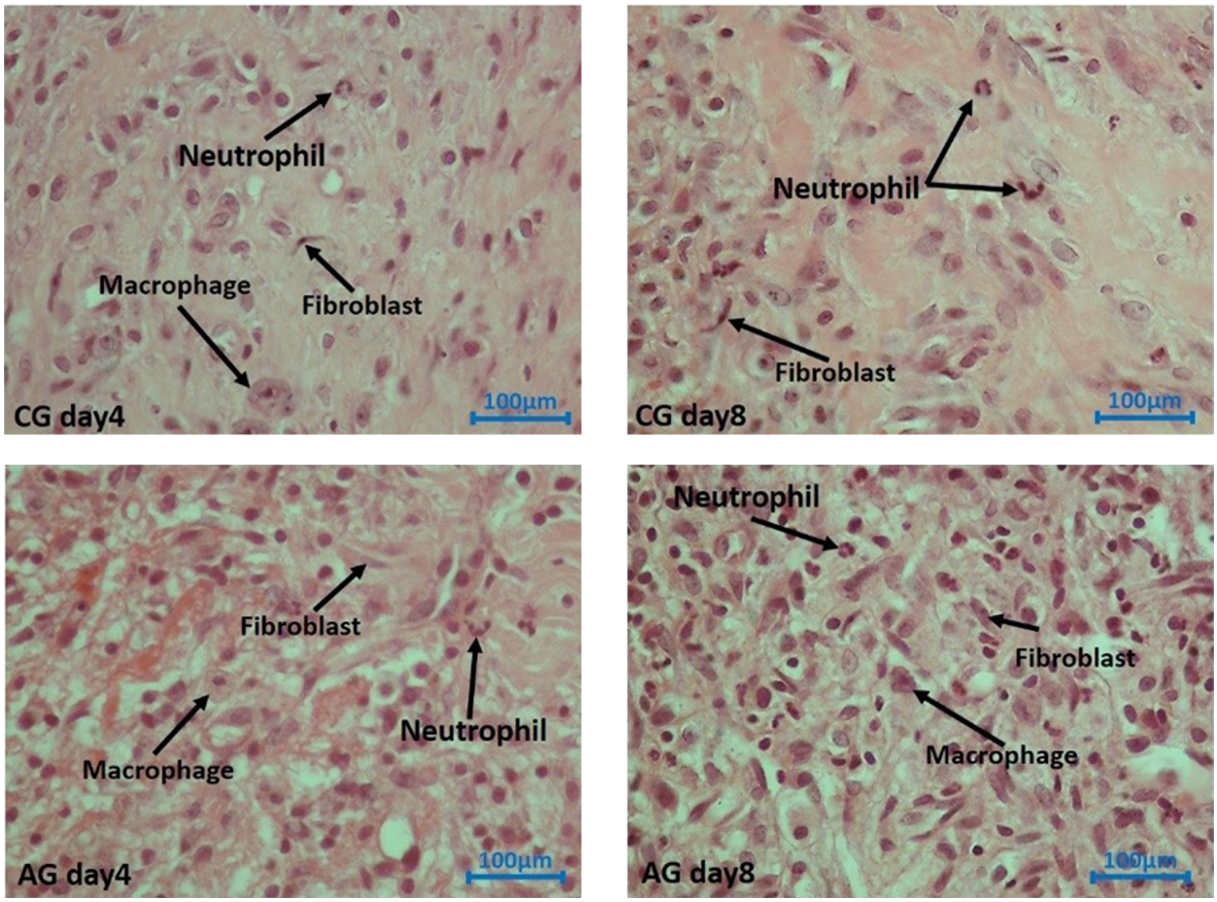

Figure 6. Hematoxylin and eosin-stained photographs of repairing tissues in all the studied groups on days 4 and 8 after surgery. CG, control group; AG, adipose-derived stem cell treatment group.

of growth factors (26, 28). It is hypothesized that ADSs may play a direct role in wound regeneration by replacing damaged cells via differentiation into epidermal cells (30). Furthermore, the findings from two relevant studies have revealed that engrafted ADSs express endothelial markers, promoting the formation of vascular networks in ischemic organs (31, 32).

In our study, we observed a significant reduction in wound area following the hADS injection, accompanied by an increase in the rate of wound closure. Notably, the administration of hADS exhibited an enhanced bactericidal effect and improved wound strength. These findings highlight the potential of ADS as an anti-inflammatory agent and support the use of ADS-based therapy in the treatment of DFUs.

Bacterial infections have been identified as the primary causative factor contributing to impaired wound healing (33). MRSA, a commonly encountered strain of staphylococcal bacteria, is responsible for numerous wound infections and has shown an alarming increase in antibiotic resistance (34). This rise and adaptation of MRSA in DFU areas (34) have resulted in an expanding spectrum of untreatable staphylococcal infections (35). Consequently, there is an urgent need for innovative approaches to combat MRSA infections and address antimicrobial resistance (AMR) concerns (36). The focus of our study was specifically to evaluate the antibacterial effects of ADS (36), as they have demonstrated antimicrobial properties in animal models.

In this study, we demonstrated that the use of ADSs can significantly decrease the microbial count compared to the control group. These findings are consistent with Lipovsky et al.'s laboratory experiment, which showed that ADS inhibits *Staphylococcus aureus* effects by generating ROS (37). The antibacterial effects of ADSs may be attributed to the induction of ROS. Kouhkheil et al. investigated the effects of CM-hBMMSC (four injections) and photobiomodulation (890 nm, 0.2 J/cm^2, 80 Hz) alone and

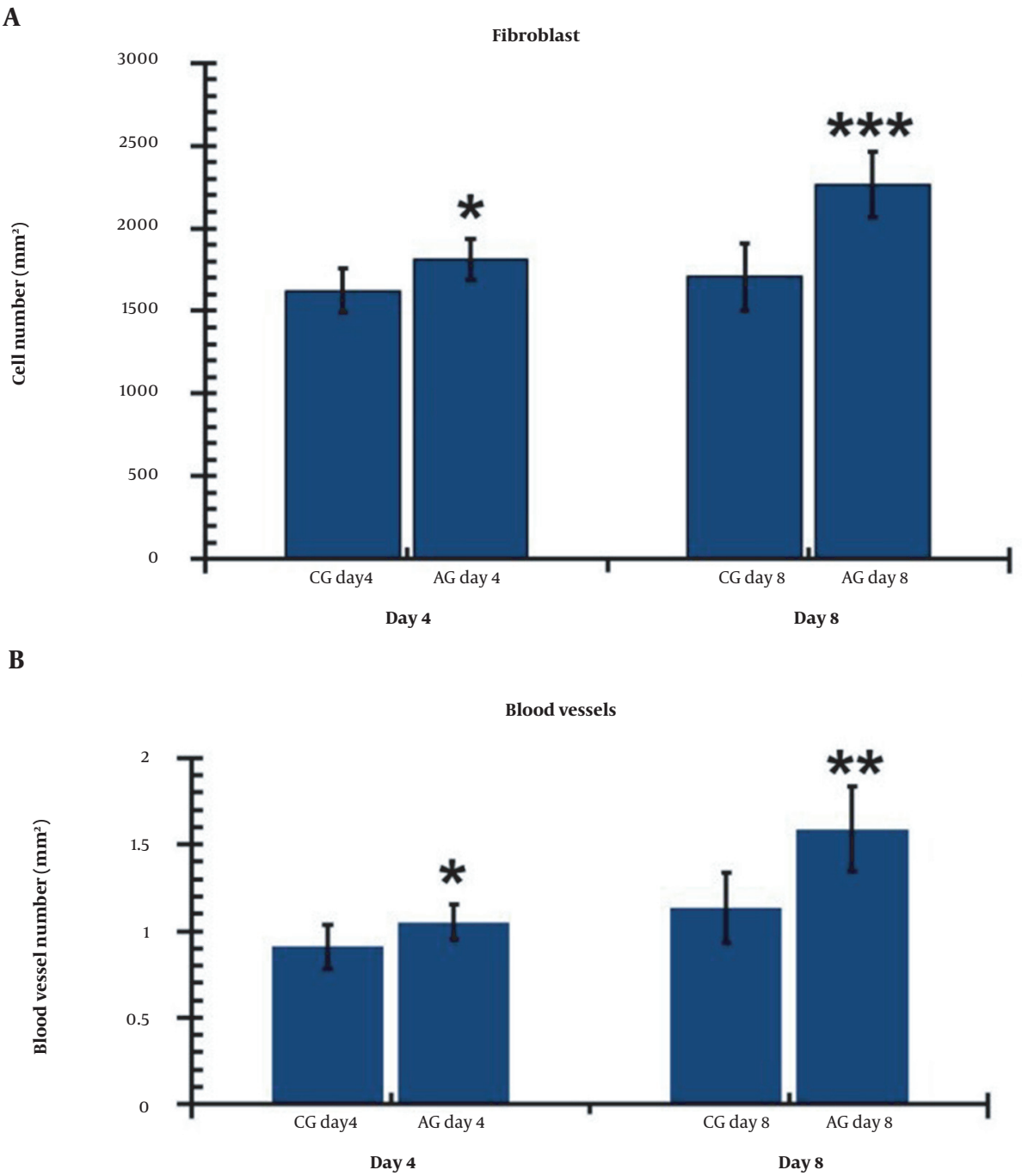

Figure 7. A, Comparison of the wounds' fibroblasts; and B, Blood vessels numbers on days 4 and 8 in the research groups. The independent-samples *t*-test and least significant difference (LSD) tests were used to examine the results, which were shown as a mean ± SD. * P < 0.05 5; ** P < 0.01; *** P < 0.001. CG, control group; AG, human adipose-derived stem cell group.

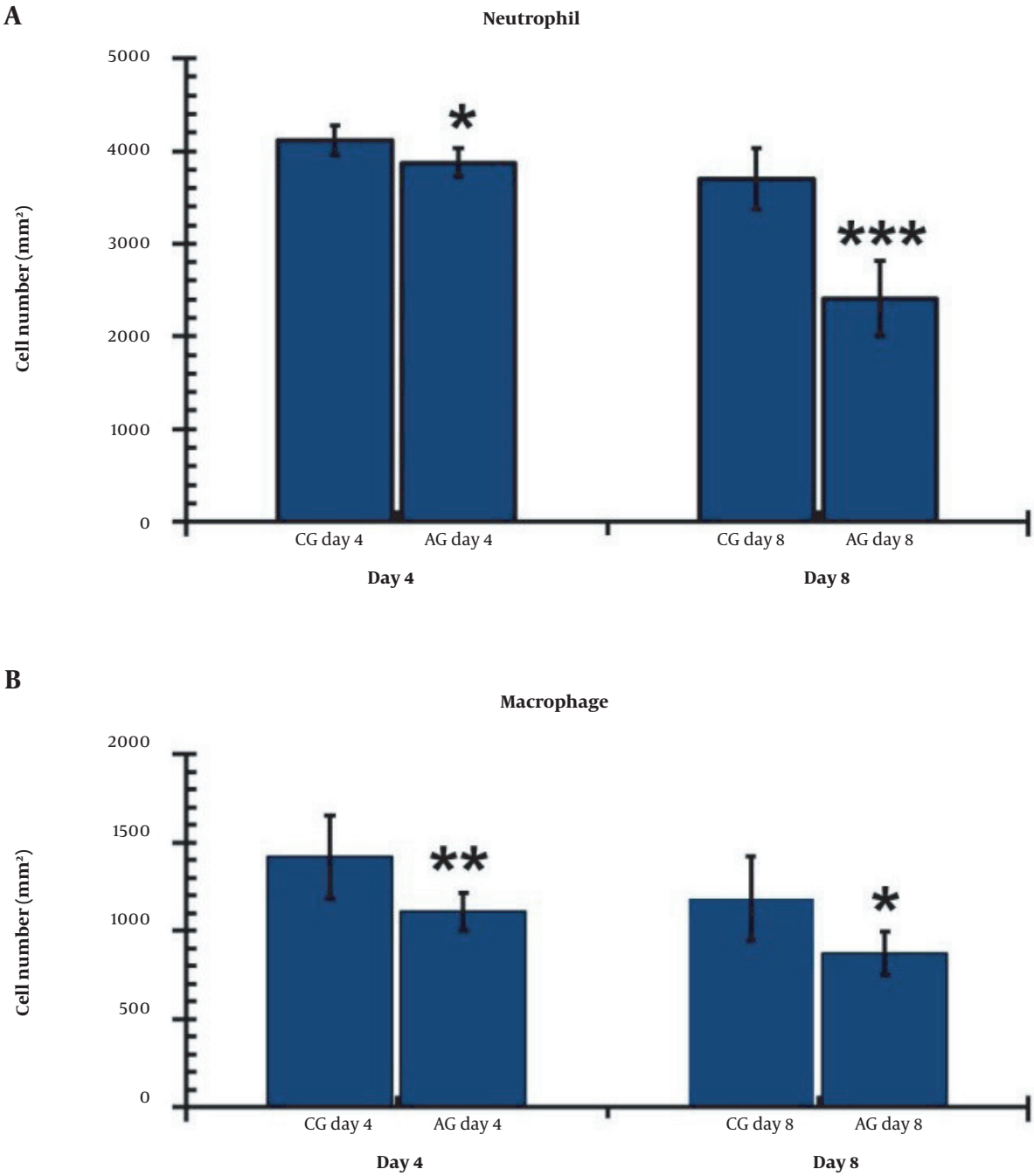

Figure 8. A, Comparison of the wounds' neutrophil; and B, Macrophage numbers on days 4 and 8 in the research groups. The independent-samples *t*-test and least significant difference (LSD) tests were used to examine the results, which were shown as a mean ± SD. * $P < 0.05$; ** $P < 0.01$; *** $P < 0.001$. CG, control group; AG, human adipose-derived stem cell group.

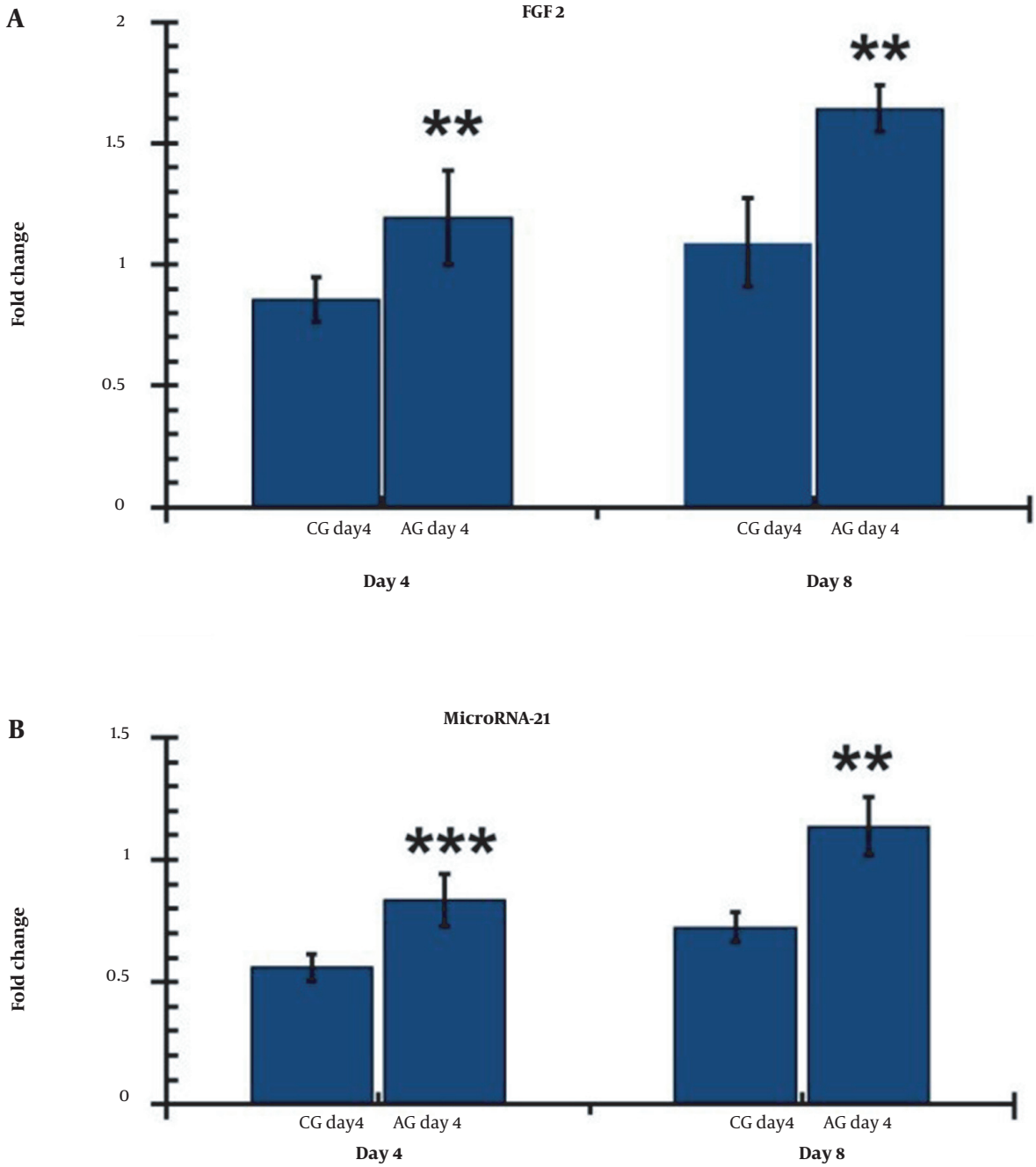

Figure 9. Comparison of FGF2 and miR-21 levels on days 4 and 8 in the damaged areas of the research groups. The independent-sample *t*-test and least significant difference (LSD) tests were used to evaluate the data, which was presented as mean standard deviation. ** $P < 0.001$; *** $P < 0.001$. CG, control group; AG, human adipose-derived stem cell group.

in combination on wound strength and CFU in an MRSA-infected wound model in DM1 rats (22).

Kouhkheil et al. demonstrated that CM-hBMMSC and PBMT, either alone or in combination, significantly reduced CFUs compared to the control group (22). In another study by Fridoni et al., the individual and combined effects of CM-hBMMSC and PBMT on stereological parameters were evaluated in an MRSA-infected wound model in rats with DM1 (38). The researchers concluded that the simultaneous use of PBMT and CM-hBMMSC had anti-inflammatory and neo-vascular effects, promoting accelerated healing of skin damage in the MRSA-infected wound model in DM1 rats (38).

DFUs are characterized by a persistent inflammatory state marked by the accumulation of inflammatory cells, pro-inflammatory cytokines, and proteases. Consistent with this, our study observed increased numbers of neutrophils and macrophages in the control group on days 4 and 8.

A study conducted by Kim et al. reported that the transition from the inflammation phase to the tissue restoration phase is crucial for effective tissue repair and renewal of ECM (39). They also highlighted the pivotal roles of endothelial and fibroblast cells in ECM remodeling and angiogenesis, which are essential for proper wound closure (39). Consistent with the findings of Kim et al., our results also demonstrated that all experimental groups had significantly higher counts of blood vessels and fibroblast cells compared to the control group, indicating enhanced angiogenesis and fibroblast activity in the treated groups (39).

In our study, the use of ADS alone demonstrated a significant increase in the levels of fibroblasts and blood vessels compared to the other experimental groups. These findings suggest that ADS treatment can effectively enhance the stereological parameters and FGF levels within ECM during the proliferative and inflammatory phases of the injury-repairing process in an infected, ischemic, and delayed wound healing model in rats with TIDM. Furthermore, the results of the stereological and FGF examinations specifically conducted in the hAD_{day8} group showed superior outcomes compared to the other groups.

FGF2 plays a crucial role in promoting endothelial cell proliferation and angiogenesis while also exerting a protective effect on endothelial cell survival. The signaling pathways involving FGF and miRNAs have been implicated in regulating various cellular processes, such as cell specification, proliferation, migration, differentiation, and survival (6).

One notable finding of our study is the expression levels of miR-21 and FGF2 genes. We observed significantly higher expression levels of miR-21 in all experimental groups compared to the control group, particularly during the proliferative phases. These results indicate that our experimental groups, especially the hAD_{day8} group, exhibited favorable performance in terms of miR-21 gene expression.

Increased expression of miR-21 increases the proliferative response, decreases the inflammatory response, and increases wound healing (40).

The administration of ADS has been shown to enhance fibroblast proliferation, increase FGF2 expression, reduce inflammation in the wound bed, and promote the transition of IIDHWM to the proliferative and remodeling phases of wound healing. These findings are consistent with both our current study and previous research. In the treatment groups, ADS treatment resulted in a significant increase in granulation tissue formation (new dermal volume) during the proliferative phase of wound healing. Furthermore, it improved tensile strength and accelerated wound closure rate during the remodeling phase (41). Based on the findings from our control group, it is evident that there is dysregulated regulation of both the inflammatory and proliferative phases in diabetic skin. This dysregulation is characterized by elevated neutrophil and macrophage counts, as well as reduced levels of miR-21 and FGF2 in the wound bed (42-44). Our research indicates that the reduced expression of miR-21 and FGF2 in the control group, which was subsequently increased by hADS therapies, may be linked to the inherent dysregulation of inflammation, proliferation, and remodeling in this group. These findings align with several relevant studies that have demonstrated the critical role of miR-21 in wound healing, as it forms a complex network with its target genes (such as PTEN, RECK, SPRY1/2, NF-B, and TIMP3) and cascaded signaling pathways (such as MAPK/ERK, PI3K/Akt, Wnt/-catenin/MMP-7, and TGF-/Smad7-Smad2/3).

The therapeutic efficacy of miR-21 may be linked to several factors, including stimulation of fibroblast differentiation, improvement of angiogenesis, anti-inflammatory effects, augmentation of collagen production, and re-epithelialization of the wound (8, 44). Xie et al. reported that miRNA-21 exerts anti-inflammatory actions and improves wound healing by regulating the expression of NF-κB via PDCD4 (8).

However, in diabetic wounds, there is a significant decline in the expression of miR-21 (8, 45, 46). The reduced levels of miR-21 are closely associated with an amplified expression level of its target gene. Therefore, increasing the level of miRNA-21 in damaged tissue can help reduce inflammatory signals and improve the healing process (45).

5.1. Conclusions

ADS-based therapies improved the inflammatory and proliferative phases of wound healing in TIDM1 rats by enhancing stereological parameters such as fibroblast cells and blood vessels, decreasing microbial counts and inflammatory elements such as neutrophils and macrophages, and increasing the expression of miRNA-21 and FGF2.

Acknowledgments

The present article is financially supported by the Research Department of the School of Medicine, Shahid Beheshti University of Medical Sciences (Grant No. 25974). The authors would like to express their sincere gratitude for their valuable support.

Footnotes

Authors' Contribution: A. A. contributed to writing the manuscript. M. B. reviewed and edited the manuscript, providing valuable comments. M. F. and M. H. conducted the experiments. A. A. performed the statistical analysis. All authors have reviewed and approved the final version of the manuscript.

Conflict of Interests: The authors declare no conflicts of interest.

Ethical Approval: The experiment was conducted with the authorization of the Medical Ethics Department of the School of Medicine, Shahid Beheshti University of Medical Sciences (SBMU), Tehran, Iran (file no. IR.SBMU.MSP.REC.1400.295).

Funding/Support: This article received financial support from Grant No. 25974 provided by the Research Department of the School of Medicine, Shahid Beheshti University of Medical Sciences.

Informed Consent: Informed consent was obtained.

References

1. American Diabetes Association. Diagnosis and classification of diabetes mellitus. *Diabetes Care*. 2004;**27 Suppl 1**:S5–S10. [PubMed ID: 14693921]. https://doi.org/10.2337/diacare.27.2007.s5.
2. Catrina SB, Zheng X. Disturbed hypoxic responses as a pathogenic mechanism of diabetic foot ulcers. *Diabetes Metab Res Rev*. 2016;**32 Suppl 1**:179–85. [PubMed ID: 26453314]. https://doi.org/10.1002/dmrr.2742.
3. Brancato SK, Albina JE. Wound macrophages as key regulators of repair: origin, phenotype, and function. *Am J Pathol*. 2011;**178**(1):19–25. [PubMed ID: 21224038]. [PubMed Central ID: PMC3069845]. https://doi.org/10.1016/j.ajpath.2010.08.003.
4. Duraisamy Y, Slevin M, Smith N, Bailey J, Zweit J, Smith C, et al. Effect of glycation on basic fibroblast growth factor induced angiogenesis and activation of associated signal transduction pathways in vascular endothelial cells: possible relevance to wound healing in diabetes. *Angiogenesis*. 2001;**4**(4):277–88. [PubMed ID: 12197473]. https://doi.org/10.1023/a:1016068917266.
5. Grazul-Bilska AT, Luthra G, Reynolds LP, Bilski JJ, Johnson ML, Adbullah SA, et al. Effects of basic fibroblast growth factor (FGF-2) on proliferation of human skin fibroblasts in type II diabetes mellitus. *Exp Clin Endocrinol Diabetes*. 2002;**110**(4):176–81. [PubMed ID: 12058341]. https://doi.org/10.1055/s-2002-32149.
6. Wolf L, Gao CS, Gueta K, Xie Q, Chevallier T, Podduturi NR, et al. Identification and characterization of FGF2-dependent mRNA: microRNA networks during lens fiber cell differentiation. *G3 (Bethesda)*. 2013;**3**(12):2239–55. [PubMed ID: 24142921]. [PubMed Central ID: PMC3852386]. https://doi.org/10.1534/g3.113.008698.
7. Li D, Landen NX. MicroRNAs in skin wound healing. *Eur J Dermatol*. 2017;**27**(S1):12–4. [PubMed ID: 28690209]. https://doi.org/10.1684/ejd.2017.3040.
8. Xie J, Wu W, Zheng L, Lin X, Tai Y, Wang Y, et al. Roles of MicroRNA-21 in Skin Wound Healing: A Comprehensive Review. *Front Pharmacol*. 2022;**13**:828627. [PubMed ID: 35295323]. [PubMed Central ID: PMC8919367]. https://doi.org/10.3389/fphar.2022.828627.
9. Bhatt K, Lanting LL, Jia Y, Yadav S, Reddy MA, Magilnick N, et al. Anti-Inflammatory Role of MicroRNA-146a in the Pathogenesis of Diabetic Nephropathy. *J Am Soc Nephrol*. 2016;**27**(8):2277–88. [PubMed ID: 26647423]. [PubMed Central ID: PMC4978034]. https://doi.org/10.1681/ASN.2015010111.
10. Sekar D, Venugopal B, Sekar P, Ramalingam K. Role of microRNA 21 in diabetes and associated/related diseases. *Gene*. 2016;**582**(1):14–8. [PubMed ID: 26826461]. https://doi.org/10.1016/j.gene.2016.01.039.
11. Liechty C, Hu J, Zhang L, Liechty KW, Xu J. Role of microRNA-21 and Its Underlying Mechanisms in Inflammatory Responses in Diabetic Wounds. *Int J Mol Sci*. 2020;**21**(9). [PubMed ID: 32397166]. [PubMed Central ID: PMC7247578]. https://doi.org/10.3390/ijms21093328.
12. Roy D, Modi A, Khokhar M, Sankanagoudar S, Yadav D, Sharma S, et al. MicroRNA 21 Emerging Role in Diabetic Complications: A Critical Update. *Curr Diabetes Rev*. 2021;**17**(2):122–35. [PubMed ID: 32359340]. https://doi.org/10.2174/1573399816666200503035035.
13. Brem H, Tomic-Canic M. Cellular and molecular basis of wound healing in diabetes. *J Clin Invest*. 2007;**117**(5):1219–22. [PubMed ID: 17476353]. [PubMed Central ID: PMC1857239]. https://doi.org/10.1172/JCI32169.
14. Moradi A, Zare F, Mostafavinia A, Safaju S, Shahbazi A, Habibi M, et al. Photobiomodulation plus Adipose-derived Stem Cells Improve Healing of Ischemic Infected Wounds in Type 2 Diabetic Rats. *Sci Rep*. 2020;**10**(1):1206. [PubMed ID: 31988386]. [PubMed Central ID: PMC6985227]. https://doi.org/10.1038/s41598-020-58099-z.
15. Hu MS, Borrelli MR, Lorenz HP, Longaker MT, Wan DC. Mesenchymal Stromal Cells and Cutaneous Wound Healing: A Comprehensive Review of the Background, Role, and Therapeutic Potential. *Stem Cells Int*. 2018;**2018**:6901983. [PubMed ID: 29887893]. [PubMed Central ID: PMC5985130]. https://doi.org/10.1155/2018/6901983.
16. Kucharzewski M, Rojczyk E, Wilemska-Kucharzewska K, Wilk R, Hudecki J, Los MJ. Novel trends in application of stem cells in skin wound healing. *Eur J Pharmacol*. 2019;**843**:307–15. [PubMed ID: 30537490]. https://doi.org/10.1016/j.ejphar.2018.12.012.
17. Gadelkarim M, Abushouk AI, Ghanem E, Hamaad AM, Saad AM, Abdel-Daim MM. Adipose-derived stem cells: Effectiveness and advances in delivery in diabetic wound healing. *Biomed Pharmacother*. 2018;**107**:625–33. [PubMed ID: 30118878]. https://doi.org/10.1016/j.biopha.2018.08.013.
18. Zhu Y, Liu T, Song K, Fan X, Ma X, Cui Z. Adipose-derived stem cell: a better stem cell than BMSC. *Cell Biochem Funct*. 2008;**26**(6):664–75. [PubMed ID: 18636461]. https://doi.org/10.1002/cbf.1488.
19. Muhammad G, Xu J, Bulte JWM, Jablonska A, Walczak P, Janowski M. Transplanted adipose-derived stem cells can be short-lived yet accelerate healing of acid-burn skin wounds: a multimodal imaging study. *Sci Rep*. 2017;**7**(1):4644. [PubMed ID: 28680144]. [PubMed Central ID: PMC5498606]. https://doi.org/10.1038/s41598-017-04484-0.

20. Mostafavinia A, Amini A, Ghorishi SK, Pouriran R, Bayat M. The effects of dosage and the routes of administrations of streptozotocin and alloxan on induction rate of type1 diabetes mellitus and mortality rate in rats. *Lab Anim Res*. 2016;**32**(3):160–5. [PubMed ID: 27729932]. [PubMed Central ID: PMC5057004]. https://doi.org/10.5625/lar.2016.32.3.160.
21. Kouhkheil R, Fridoni M, Piryaei A, Taheri S, Chirani AS, Anarkooli IJ, et al. The effect of combined pulsed wave low-level laser therapy and mesenchymal stem cell-conditioned medium on the healing of an infected wound with methicillin-resistant Staphylococcal aureus in diabetic rats. *J Cell Biochem*. 2018;**119**(7):5788–97. [PubMed ID: 29574990]. https://doi.org/10.1002/jcb.26759.
22. Kouhkheil R, Fridoni M, Abdollhifar MA, Amini A, Bayat S, Ghoreishi SK, et al. Impact of Photobiomodulation and Condition Medium on Mast Cell Counts, Degranulation, and Wound Strength in Infected Skin Wound Healing of Diabetic Rats. *Photobiomodul Photomed Laser Surg*. 2019;**37**(11):706–14. [PubMed ID: 31589095]. https://doi.org/10.1089/photob.2019.4691.
23. Moradi A, Kheirollahkhani Y, Fatahi P, Abdollahifar MA, Amini A, Naserzadeh P, et al. An improvement in acute wound healing in mice by the combined application of photobiomodulation and curcumin-loaded iron particles. *Lasers Med Sci*. 2019;**34**(4):779–91. [PubMed ID: 30393833]. https://doi.org/10.1007/s10103-018-2664-9.
24. Nourian Dehkordi A, Mirahmadi Babaheydari F, Chehelgerdi M, Raeisi Dehkordi S. Skin tissue engineering: wound healing based on stem-cell-based therapeutic strategies. *Stem Cell Res Ther*. 2019;**10**(1):111. [PubMed ID: 30922387]. [PubMed Central ID: PMC6440165]. https://doi.org/10.1186/s13287-019-1212-2.
25. Hassan WU, Greiser U, Wang W. Role of adipose-derived stem cells in wound healing. *Wound Repair Regen*. 2014;**22**(3):313–25. [PubMed ID: 24844331]. https://doi.org/10.1111/wrr.12173.
26. Gonzalez MA, Gonzalez-Rey E, Rico L, Buscher D, Delgado M. Adipose-derived mesenchymal stem cells alleviate experimental colitis by inhibiting inflammatory and autoimmune responses. *Gastroenterology*. 2009;**136**(3):978–89. [PubMed ID: 19135996]. https://doi.org/10.1053/j.gastro.2008.11.041.
27. Periasamy R, Elshaer SL, Gangaraju R. CD140b (PDGFRbeta) signaling in adipose-derived stem cells mediates angiogenic behavior of retinal endothelial cells. *Regen Eng Transl Med*. 2019;**5**(1):1–9. [PubMed ID: 30976657]. [PubMed Central ID: PMC6453132]. https://doi.org/10.1007/s40883-018-0068-9.
28. Sumi M, Sata M, Toya N, Yanaga K, Ohki T, Nagai R. Transplantation of adipose stromal cells, but not mature adipocytes, augments ischemia-induced angiogenesis. *Life Sci*. 2007;**80**(6):559–65. [PubMed ID: 17157325]. https://doi.org/10.1016/j.lfs.2006.10.020.
29. Harada Y, Yamamoto Y, Tsujimoto S, Matsugami H, Yoshida A, Hisatome I. Transplantation of freshly isolated adipose tissue-derived regenerative cells enhances angiogenesis in a murine model of hind limb ischemia. *Biomed Res*. 2013;**34**(1):23–9. [PubMed ID: 23428977]. https://doi.org/10.2220/biomedres.34.23.
30. Li P, Guo X. A review: therapeutic potential of adipose-derived stem cells in cutaneous wound healing and regeneration. *Stem Cell Res Ther*. 2018;**9**(1):302. [PubMed ID: 30409218]. [PubMed Central ID: PMC6225584]. https://doi.org/10.1186/s13287-018-1044-5.
31. Miyahara Y, Nagaya N, Kataoka M, Yanagawa B, Tanaka K, Hao H, et al. Monolayered mesenchymal stem cells repair scarred myocardium after myocardial infarction. *Nat Med*. 2006;**12**(4):459–65. [PubMed ID: 16582917]. https://doi.org/10.1038/nm1391.
32. Nakagami H, Maeda K, Morishita R, Iguchi S, Nishikawa T, Takami Y, et al. Novel autologous cell therapy in ischemic limb disease through growth factor secretion by cultured adipose tissue-derived stromal cells. *Arterioscler Thromb Vasc Biol*. 2005;**25**(12):2542–7. [PubMed ID: 16224047]. https://doi.org/10.1161/01.ATV.0000190701.92007.6d.
33. Edwards R, Harding KG. Bacteria and wound healing. *Curr Opin Infect Dis*. 2004;**17**(2):91–6. [PubMed ID: 15021046]. https://doi.org/10.1097/00001432-200404000-00004.
34. Boulton AJM, Armstrong DG, Kirsner RS, Attinger CE, Lavery LA, Lipsky BA, et al. *Diagnosis and Management of Diabetic Foot Complications*. Arlington, USA: ADA Clinical Compendia; 2018. eng. https://doi.org/10.2337/db20182-1.
35. Smith TL, Pearson ML, Wilcox KR, Cruz C, Lancaster MV, Robinson-Dunn B, et al. Emergence of vancomycin resistance in Staphylococcus aureus. Glycopeptide-Intermediate Staphylococcus aureus Working Group. *N Engl J Med*. 1999;**340**(7):493–501. [PubMed ID: 10021469]. https://doi.org/10.1056/NEJM199902183400701.
36. Mot YY, Othman I, Sharifah SH. Synergistic antibacterial effect of co-administering adipose-derived mesenchymal stromal cells and Ophiophagus hannah L-amino acid oxidase in a mouse model of methicillin-resistant Staphylococcus aureus-infected wounds. *Stem Cell Res Ther*. 2017;**8**(1):5. [PubMed ID: 28114965]. [PubMed Central ID: PMC5259957]. https://doi.org/10.1186/s13287-016-0457-2.
37. Lipovsky A, Nitzan Y, Gedanken A, Lubart R. Visible light-induced killing of bacteria as a function of wavelength: implication for wound healing. *Lasers Surg Med*. 2010;**42**(6):467–72. [PubMed ID: 20662022]. https://doi.org/10.1002/lsm.20948.
38. Fridoni M, Kouhkheil R, Abdollhifar MA, Amini A, Ghatrehsamani M, Ghoreishi SK, et al. Improvement in infected wound healing in type 1 diabetic rat by the synergistic effect of photobiomodulation therapy and conditioned medium. *J Cell Biochem*. 2019;**120**(6):9906–16. [PubMed ID: 30556154]. https://doi.org/10.1002/jcb.28273.
39. Kim H, Kim DE, Han G, Lim NR, Kim EH, Jang Y, et al. Harnessing the Natural Healing Power of Colostrum: Bovine Milk-Derived Extracellular Vesicles from Colostrum Facilitating the Transition from Inflammation to Tissue Regeneration for Accelerating Cutaneous Wound Healing. *Adv Healthc Mater*. 2022;**11**(6). e2102027. [PubMed ID: 34865307]. https://doi.org/10.1002/adhm.202102027.
40. Madhyastha R, Madhyastha H, Nakajima Y, Omura S, Maruyama M. MicroRNA signature in diabetic wound healing: promotive role of miR-21 in fibroblast migration. *Int Wound J*. 2012;**9**(4):355–61. [PubMed ID: 22067035]. [PubMed Central ID: PMC7950390]. https://doi.org/10.1111/j.1742-481X.2011.00890.x.
41. Ahmadi H, Amini A, Fadaei Fathabady F, Mostafavinia A, Zare F, Ebrahimpour-Malekshah R, et al. Transplantation of photobiomodulation-preconditioned diabetic stem cells accelerates ischemic wound healing in diabetic rats. *Stem Cell Res Ther*. 2020;**11**(1):494. [PubMed ID: 33239072]. [PubMed Central ID: PMC7688005]. https://doi.org/10.1186/s13287-020-01967-2.
42. Geiger A, Walker A, Nissen E. Human fibrocyte-derived exosomes accelerate wound healing in genetically diabetic mice. *Biochem Biophys Res Commun*. 2015;**467**(2):303–9. [PubMed ID: 26454169]. https://doi.org/10.1016/j.bbrc.2015.09.166.
43. Roy S, Sen CK. miRNA in wound inflammation and angiogenesis. *Microcirculation*. 2012;**19**(3):224–32. [PubMed ID: 22211762]. [PubMed Central ID: PMC3399420]. https://doi.org/10.1111/j.1549-8719.2011.00156.x.
44. Trzyna A, Banas-Zabczyk A. Adipose-Derived Stem Cells Secretome and Its Potential Application in "Stem Cell-Free Therapy". *Biomolecules*. 2021;**11**(6). [PubMed ID: 34199330]. [PubMed Central ID: PMC8231996]. https://doi.org/10.3390/biom11060878.
45. Li Q, Zhao H, Chen W, Huang P, Bi J. Human keratinocyte-derived microvesicle miRNA-21 promotes skin wound healing in diabetic rats through facilitating fibroblast function and angiogenesis. *Int J Biochem Cell Biol*. 2019;**114**:105570. [PubMed ID: 31302227]. https://doi.org/10.1016/j.biocel.2019.105570.
46. Raziyeva K, Kim Y, Zharkinbekov Z, Kassymbek K, Jimi S, Saparov A. Immunology of Acute and Chronic Wound Healing. *Biomolecules*. 2021;**11**(5). [PubMed ID: 34066746]. [PubMed Central ID: PMC8150999]. https://doi.org/10.3390/biom11050700.